Article

Rapid and Effective Sample Cleanup Based on Polyvinylpyrrolidone-Coated Magnetite Nanoparticles Coupled with New Pre-Column Derivatization for Determination of Aflatoxins B_1, B_2, G_1 and G_2 in Animal Feeds by High-Performance Liquid Chromatography with Fluorescence Detection

Jiao Zhao, [*,a,b] *Yifang Zhou,[a] Yi Zhang,[a] Baoling Wang[a] and Dandan Ge [a]*

*[a]Department of Chemical Science and Technology, Kunming University,
650214 Kunming, Yunnan Province, P. R. China*

*[b]Yunnan Key Laboratory of Food-Safety Testing Technology, Kunming University,
650214 Kunming, Yunnan Province, P. R. China*

A novel method for the determination of aflatoxins B_1, B_2, G_1, and G_2 (AFB$_1$, AFB$_2$, AFG$_1$, AFG$_2$) in animal feed samples based on magnetic solid-phase cleanup and novel pre-column derivatization has been developed. In this work, synthesized polyvinylpyrrolidone-coated Fe$_3$O$_4$ magnetic nanoparticles were applied as adsorbents for rapid cleanup for extracts of animal feed samples. The purified extract was then derivatized with trifluoroacetic acid coupling ultraviolet irradiation which enabled the weakly fluorescent AFB$_1$ and AFG$_1$ transformed into their highly fluorescent hemiacetals derivatives. Afterward aflatoxins were separated and quantified by reverse phase liquid chromatography with fluorescence detection. The results indicated that four AFs presented excellent linear response with correlation coefficients > 0.996 and recoveries ranged from 86.7 to 108.9% with relative standard deviations (RSDs) from 3.6 to 6.4%. The limits of detection (LODs) were 0.0392, 0.2429, 0.0842, 0.4556 ng mL^{-1} for AFB$_1$, AFB$_2$, AFG$_1$ and AFG$_2$, respectively.

Keywords: aflatoxins, magnetic solid-phase cleanup, pre-column derivatization, reverse phase liquid chromatography with fluorescence detection, animal feed

Introduction

Naturally occurring, aflatoxins B_1, B_2, G_1, and G_2 (AFB$_1$, AFB$_2$, AFG$_1$, AFG$_2$) are secondary metabolites of the molds *Aspergillus flavus* and *Aspergillus parasiticus*.[1-3] They are highly toxic, mutagenic, teratogenic and carcinogenic compounds found to contaminate a wide variety of important agricultural products such as peanuts, maize, rice, tree nuts and spices.[4-7] Since animal feed utilizes these agricultural crops, contamination of aflatoxins poses a risk to animal health and the consumption of polluted feed is also derived from the contamination of foods of animal origin such as meat, milk and other dairy products. However, animal feed has complicated compositions such as starches, vitamins, fats and other chemicals, which challenges the analyses of aflatoxins in animal feed.

In the past decades, many kinds of efforts have been made to enable analysis of aflatoxins in complex matrices. Generally, the most common sample treatment used for the

determination of aflatoxins in animal feed involves the use of sample extraction followed by a cleanup step. The cleanup steps can minimize the influence of matrix components and improve accuracy of detection. When purification and cleanup are required, liquid-liquid extraction[8,9] or, more recently, solid-phase extraction cartridges,[10-12] immunoaffinity column[13-15] and multifunctional purification column[16-18] are usually used. Although immunoaffinity column and multifunctional purification column have excellent analyte selectivity, they are expensive and tedious to use. And, liquid-liquid extraction and solid-phase dispersion are time consuming and complicated for analyzing aflatoxins in animal feeds. Developing an efficient and low cost material which produces reliable data, good purification effect and reproducible results is of imminent interest to researchers. In this present work, synthesized polyvinylpyrrolidone-coated magnetite Fe$_3$O$_4$ nanoparticles (PVP@Fe$_3$O$_4$ NPs) were used as cleanup adsorbent in the sample purification for its simplicity of operating, time saving, low cost and availability. The matrix interferences are partitioned from the sample matrix and adsorbed on

the surface of magnetite nanoparticles (MNPs) to purify sample solution. On account of the polyvinylpyrrolidone (PVP) shell that endows the magnetic sorbent with highly efficient cleanup performance and protects the Fe_3O_4 core against oxidation and aggregation,[19,20] the as-prepared PVP@Fe_3O_4 NPs can effectively reduce and even eliminate the matrix effect in feed samples, without adsorbing the target AFs. Subsequently, the PVP@Fe_3O_4 NPs that adsorb impurities can be readily isolated from sample solutions by application of an external magnetic field without additional centrifugation or filtration of the sample, which makes purification and separation easier and faster.[21]

The determination of these toxins is not easy because they have been found in complex matrices and should be detected in low concentrations. Among different analytical methods available, high-performance liquid chromatography with fluorescence detection (HPLC-FLD) is currently the most widely used for the determination of aflatoxins due to its great versatility in the analysis of complex matrices.[22,23] However, it usually cannot give a satisfactory result for the fluorescence emissions of AFB_1 and AFG_1 which were markedly quenched by eluents used in both normal and reversed-phase (RP) HPLC. In order to produce the highly fluorescent derivatives AFB_{2a} and AFG_{2a} from the less fluorescent AFB_1 and AFG_1, respectively, the native fluorescence of AFB_1 and AFG_1 has been enhanced by different derivatization procedures: pre-column formation of hemiacetal derivates with trifluoracetic acid (TFA) or post-column derivatization with bromine or iodine (directly added or electrochemically cell produced).[24-26] Although these methods produce molecules with fluorescence intensity higher than their precursors, they also present several disadvantages. The major disadvantage of TFA derivatization is the low stability of AFB_1 and AFG_1 derivatives in methanol probably due to the formation of methyl acetals.[27] The iodine derivatization also presents several drawbacks: the formation of numerous secondary products, dilution caused by reagent addition, the iodine solution must be prepared daily for stability reasons, an additional pump is needed and the use of very saturated solutions contributes to the great physical and mechanic deterioration of the connection tubing and the post-column pumping device suffers, owing to its prolonged contact with iodine. Post-column photochemical derivatization (PD) enhancement of fluorescence is desirable because it offers an easily controlled online step, but it needs special instruments that limit its popularization and application.

In this work, AFB_1 and AFG_1 derivatives were obtained by adding TFA to the sample solution and radiating 15 min by UV lamp simultaneously. The results showed that AFB_1 and AFG_1 derivatives are far more fluorescent than their unsaturated homologues and no effect was observed on AFB_2 and AFG_2. The combination of TFA with UV irradiation not only reveals the advantages of not requiring expensive equipment such as electrochemical genera system, additional pumps or photochemical reactor, but also improves the stability of AFB_1 and AFG_1 derivatives.

The aim of the present work are: (*i*) to synthesize an easy control and low cost magnetic sorbent for solid-phase clean-up of extracted feed samples; (*ii*) to develop a new pre-column derivatization method coupled with HPLC-FLD for sensitive and reliable analysis of AFs (AFB_1, AFB_2, AFG_1, AFG_2) in animal feeds. The main experimental parameters affecting the two-step pretreatment procedures were investigated in details and the analytical characteristics of the method were evaluated. The method has been fully validated on three animal feed samples.

Experimental

Instrumentation

HPLC analysis was performed with an Agilent 1260 HPLC system (Agilent Technologies, Germany) equipped with a quaternary pump, an automatic sample injector, a degasser, and a fluorescence detector. Chromatographic separations were performed on a reversed phase C_{18} analytical column (150 × 4.6 mm, 5 μm, Agilent) at 25 °C, with an isocratic elution of methanol-water (45:55, v/v) at a flow rate of 1 mL min^{-1}. The injection volume was 20 μL. The detection wavelengths were 365 and 440 nm for excitation and emission, respectively. Scanning electron microscopy (SEM) scanning system VEGA3 SBH (Tescan, Czech Republic) with a tungsten electron gun and transmission electron microscope (TEM) scanning system JEM-100CXII (Japan Electronics Co., Japan) were used for characterization of MNPs. A vortex mixer (Shanghai, China) was used to mix and accelerate the reactions between reagents. UV irradiation was provided by a 9 W UV lamp (Kunming, Yunnan).

Materials

All reagents used were analytical or chromatographic grade. AF standards including AFB_1, AFB_2, AFG_1 and AFG_2 were purchased from Sigma-Aldrich (St. Louis, USA). The structures of the four AFs were shown in Figure 1. Stock standard solutions (200 ng mL^{-1} AFB_1, 500 ng mL^{-1} AFB_2, 200 ng mL^{-1} AFG_1, and 500 ng mL^{-1} AFG_2) and working standard solutions were prepared in acetonitrile and stored at 4 °C in brown glass vials. Analytical-grade TFA was purchased from Shanghai Cheng Jie Chemical, China. Ferric chloride ($FeCl_3 \cdot 6H_2O$) and ammonia solution were

purchased from Tianjinzhiyuan Chemical Reagen Co. Ltd. (Tianjin, China). Ammonium iron (II) sulfate hexahydrate $((NH_4)_2Fe(SO_4)_2 \cdot 6H_2O)$, acetonitrile and methanol were purchased from Guangzhou Jinhuada Chemical Reagent Co., Ltd. (Guangzhou, China). PVP was purchased from Aladdin Chemical Co. Ltd. (Shanghai, China).
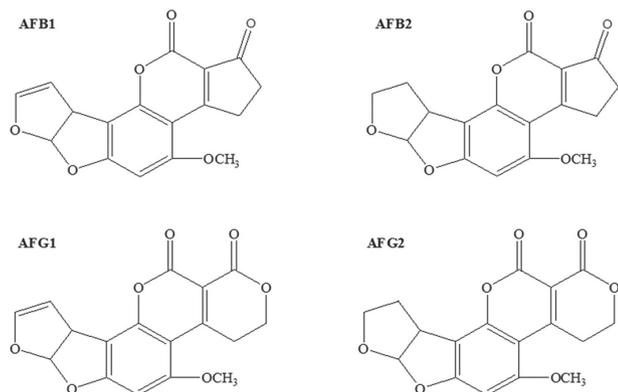
Figure 1. Chemical structures of AFB_1, AFB_2, AFG_1 and AFG_2.

Preparation of polyvinylpyrrolidone-coated Fe_3O_4 magnetic nanoparticles

The Fe_3O_4 nanoparticles were synthesized using a modified co-precipitation method in air rather than an inert atmosphere as previously performed. To prepare PVP@Fe_3O_4 NPs,[28] 0.18 mmol PVP was added to 6.25 mL ultrapure water while the solution was stirred at 80 °C. After that, 1 mmol $FeCl_2 \cdot 4H_2O$ and 4 mmol $FeCl_3 \cdot 6H_2O$ were added to the solution and stirred at 80 °C. In the next step, 0.12 mmol PVP was dissolved in the solution. Finally, 6.25 mL ammonia solution was added into the solution dropwise at room temperature with vigorous stirring. After the addition of ammonia solution, the color of the mixture turned from yellow to black immediately and the black suspension was allowed to mix for 25 min at 90 °C. The precipitates were isolated from the supernatant solution by an external supermagnet and washed once with deionized water. The obtained PVP@Fe_3O_4 NPs were redispersed in 50 mL of deionized water via sonication and the concentration of PVP@Fe_3O_4 NPs suspension was estimated to be about 50 mg mL^{-1}.

Samples preparation

Feed samples of different kinds of livestock (pig, chicken and fish) were purchased from local supermarkets (Yunnan, China) and stored at room temperature. Before the analysis, 50 g samples were milled and homogenized using a standard grinder (Jiangsu, China). For extraction of analytes, 5.0 g of prepared sample powder were added to a 50 mL centrifuge tube and ultrasonically extracted with 20 mL of a mixture of MeOH/water (80:20, v/v). The mixture was then centrifuged at 4000 rpm for 5 min. The supernatant was collected and the residue was again extracted with 20 mL MeOH/water (80:20, v/v) and centrifuged. The supernatants were combined and diluted to 50 mL with ultrapure water for subsequent cleanup procedure.

Magnetic solid-phase clean-up and pre-column derivatization

An aliquot of 600 μL of PVP@Fe_3O_4 NPs were put into the sample solution and the mixture was ultrasonicated for 2 min. The magnetic nanoparticles were separated by a Nd-Fe-B magnet (magnetic induction intensity about 3100 Gauss) on the outer wall of the conical flask and the supernatant was decanted into a new 50 mL glass tube. The purified AFs-contained supernatant was evaporated under a gentle stream of nitrogen. After then, the residual was diluted to 0.8 mL with acetonitrile and 120 μL TFA was added. Finally, the mixture was filtered with 0.45 μm nylon membrane filter into chromatographic sample bottle and was placed under UV light irradiation of 365 nm for 15 min.

Immunoaffinity column cleanup

In order to compare with the proposed method, 10.0 mL feed sample extract was passed through the immunoaffinity column (IAC) at a flow rate of 1-2 drops *per* second. The column was rinsed twice with 10 mL of water followed by drying of the column with air forced through the column. Aflatoxins were then eluted with 3 × 1.0 mL acetonitrile into a 10 mL glass tube and were evaporated under a gentle stream of nitrogen to nearly dryness. The final solution was evaporated to 1 mL under nitrogen flow and filtered with 0.45 μm nylon membrane filter before injection into HPLC-FLD system.

Derivatization design and statistical analysis

In traditional methods, derivatization parameters are optimized by one-factor-at-a-time experiments. This procedure is troublesome and time-consuming as well as it ignores the interaction effect of parameters. Compared to the classical methods, response surface methodology (RSM) is more efficient, requires fewer data and provides interaction effects on the response besides factor effects. Three factors including the amount of TFA, reaction temperature and UV radiation time, were chosen based on single-factor designs for further optimisation by employing a three-level, three-variable Box-Behnken design (BBD) from RSM. AFB_1 and AFG_1 were used as standards of the tested compounds.

A software Design-Expert 7.1.3[29] was used to obtain the coefficients of the quadratic polynomial model. The quality of the fitted model was expressed by the coefficient of determination (R^2), and its statistical significance was checked by an *F*-test.

Results and Discussion

Characterization of PVP@Fe₃O₄ NPs

The morphology and dimension of the prepared Fe_3O_4 and PVP@Fe_3O_4 nanoparticles were explored by SEM and TEM techniques. The SEM-images of synthesized nanoparticles (Figure 2) showed homogeneous distributions of particles and that the particle sizes for the nanoparticles were between 100 and 300 nm and they tended to aggregate to larger particles, which is attributed to their large specific surface area and

high surface energy. As shown in Figure 3, the prepared PVP@Fe_3O_4 nanoparticles are nearly spherical in shape with a diameter of about 20 nm and the edge morphology of PVP@Fe_3O_4 (Figure 3b) became blurred compared with bare Fe_3O_4 NPs (Figure 3a), because the particles' surface was encapsulated with PVP. The prepared PVP@Fe_3O_4 NPs were prevented from agglomeration by a monolayer of PVP.

Optimization of magnetic solid-phase cleanup

During the sample pretreatment procedure, several parameters affect the cleaning efficiency and the AFs recoveries were investigated. Therefore, various conditions such as sample pH, amount of adsorbent and cleanup time were investigated to achieve the optimal sample pretreatment. Experiments were carried out with feed sample spiked with 20.00 ng g⁻¹ of each AF.
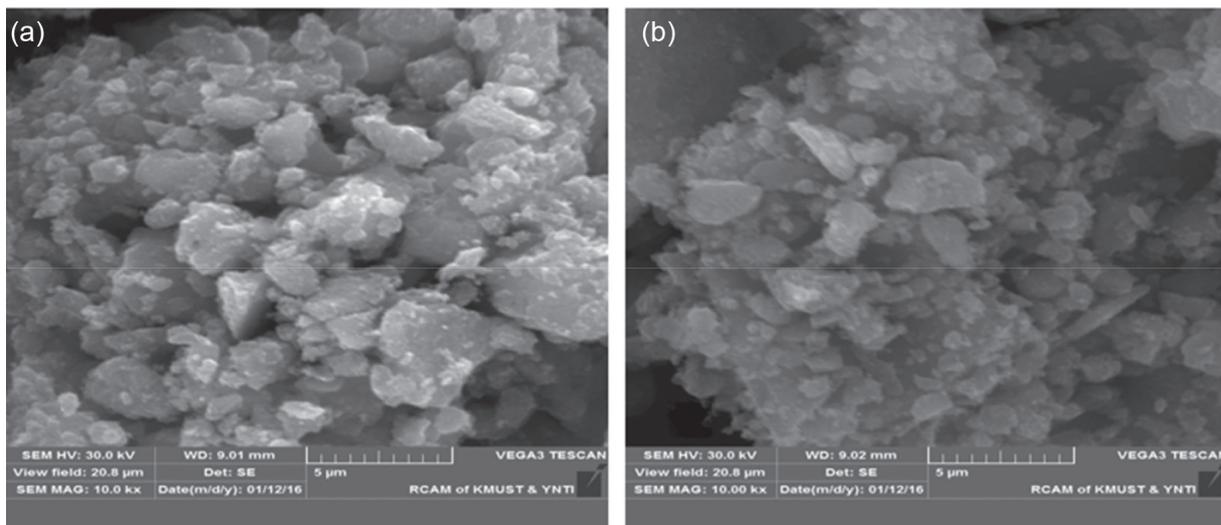
Figure 2. SEM images of Fe₃O₄ NPs (a) and PVP@Fe₃O₄ NPs (b).
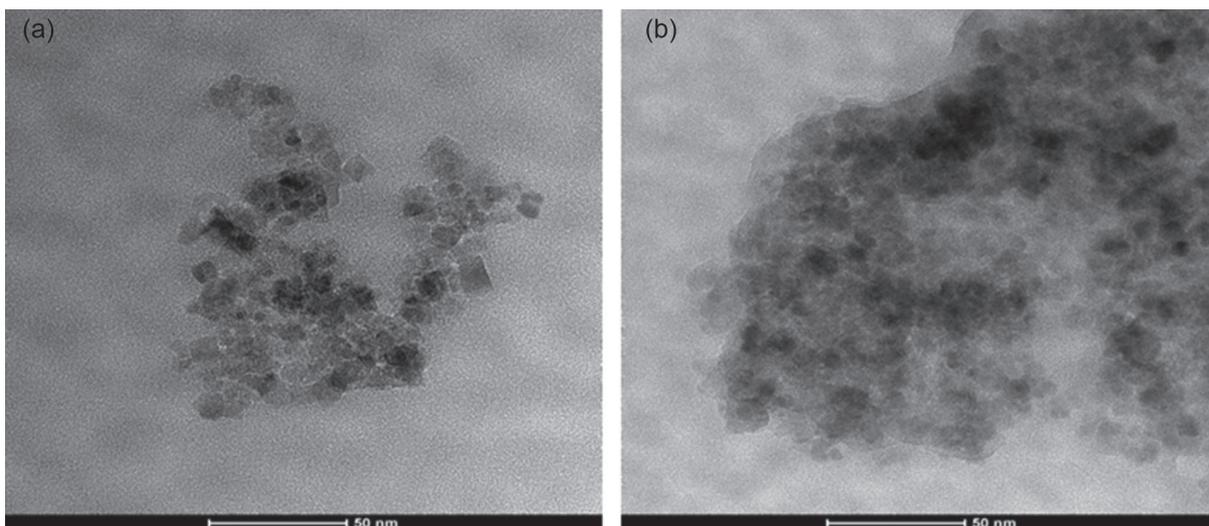
Figure 3. TEM images of Fe₃O₄ NPs (a) and PVP@Fe₃O₄ NPs NPs (b).

Effect of sample pH

Generally, solution pH may play a key role in the cleanup process because it would affect the state of target analytes and impurity substances, as well as the surface charge of adsorbents. In this work, the pH effect was examined varying from 3.0 to 11.0, and the results were shown in Figure 4. It can be seen that poor recoveries were obtained when sample solutions were acidic. With the pH increasing, the recoveries of AFs increased and reached plateau values with pH closing to 7.0. In this work, we use methanol/water (80:20, v/v) as extractant whose pH was about 7.0, and the cleanup process was carried out by directly adding $PVP@Fe_3O_4$ into the extraction solvent without pH adjustment. Therefore, there was no need to adjust the pH of the sample solution.
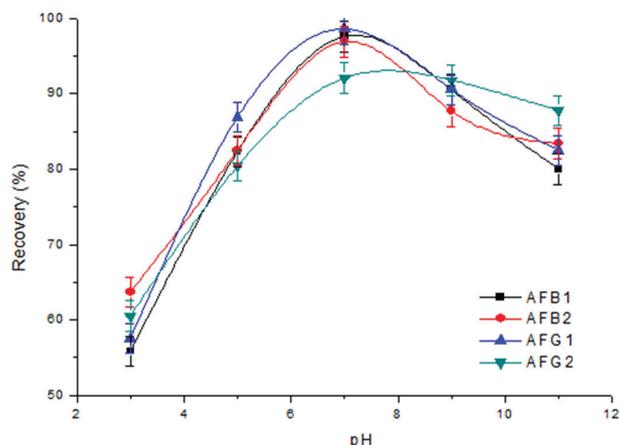
Figure 4. Effect of sample pH.

Effect of cleanup adsorbent amount

To obtain the maximum purification efficiencies of magnetic cleanup, the amount of cleanup adsorbents was optimized by varying amounts of $PVP@Fe_3O_4$ NPs from 10 to 50 mg. The effect of various amounts of $PVP@Fe_3O_4$ NPs on cleanup efficiency and AFs recoveries was investigated. The spiked extracts were purified by employing different amounts of $PVP@Fe_3O_4$ NPs, and the results were shown in Figure 5. It can be seen that the dispersive $PVP@Fe_3O_4$ adsorbent had an obvious influence on the recoveries of the target AFs, when it was increased the amount of adsorbent ranging from 10 to 50 mg. When 10 to 20 mg of $PVP@Fe_3O_4$ NPs were used for cleanup procedure, poor recoveries of AFs were obtained in range of 46.3-70.5%, which may be contributed to matrix inhibition result. With the increase of the amount of $PVP@Fe_3O_4$ from 30 to 50 mg, relative recoveries of the AFs were consistently in range of 86.9-108.2%. It was observed that the least amount of $PVP@Fe_3O_4$ adsorbent of 40 mg can effectively remove various matrices. Considering economy, the least amount (40 mg) of $PVP@Fe_3O_4$ adsorbent was selected for efficient and simple cleanup while maintaining quantitative recovery of the target AFs.
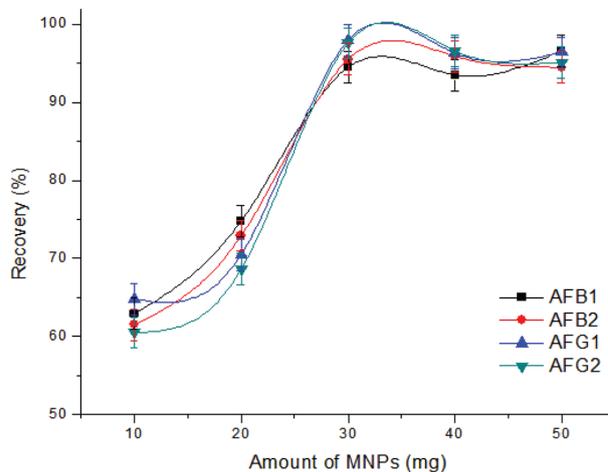
Figure 5. Effect of adsorbent amount.

Subsequently, the condition of impurities adsorption time was also investigated. To increase the precision and sensitivity of the purification procedure, it is necessary to select an exposure time that guarantees the equilibrium between aqueous phase and sorbent. It is well-known that ultrasonic process is an effective way to enhance mass transfer process in the complex matrix. In order to analyze the effect of adsorption time on the recovery of the analytes, the ultrasound time was investigated in the range of 2 to 10 min. No significant influence on the recoveries was observed. The results showed that 2 min with the assistance of ultrasonic was sufficient for impurity removal of extract sample which are more convenient and efficient than the traditional column-passing solid-phase extraction (SPE) clean up.

Optimization of pre-column derivatization

Effect of derivatizing reagent

The conversions of AFB_1 to AFB_{2a}, AFG_1 to AFG_{2a} in aqueous TFA are well established.[30] It was hoped that adding acid to the sample extract might increase the conversions during the photolysis. By combination of acid and UV light, aflatoxin hemiacetals derivatives (AFB_{2a}, AFG_{2a}) were obtained with far more fluorescence intensity than their unsaturated homologues (AFB_1, AFG_1). The derivatization scheme of AFB_1 and AFG_1 is shown in Figure 6.[31] In this study five different kinds of acids as derivatizing reagent (HNO_3, HCl, H_2SO_4, CH_3COOH, TFA) were studied for pre-derivatization of AFB_1 and AFG_1. The peak areas were investigated with the feed sample spiked

with 20.00 ng g^{-1} each AF. After acid was introduced to the purified sample, the mixture was exposed to the UV radiation. Little fluorescence intensity enhancement was achieved by directing photocatalysis as shown in Figure 7, and indicated that the derivatization reaction depended on acid. When TFA was used, the largest derivatization yield and fastest reaction time were showed compared to the other derivatization reagents. So, TFA was selected for further investigation. The derivatization reaction by TFA is fast and mild, and produces only one product.
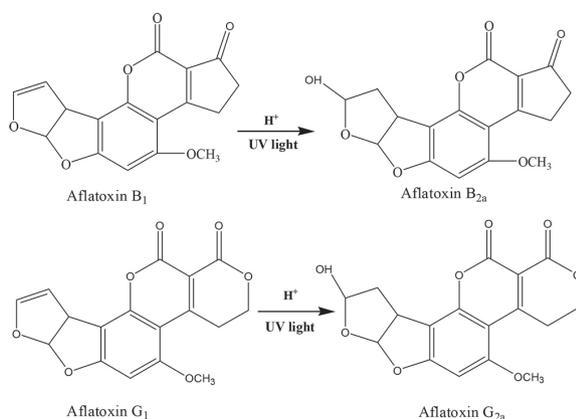
Figure 6. Structures of the B$_1$, G$_1$ and their hydration products.
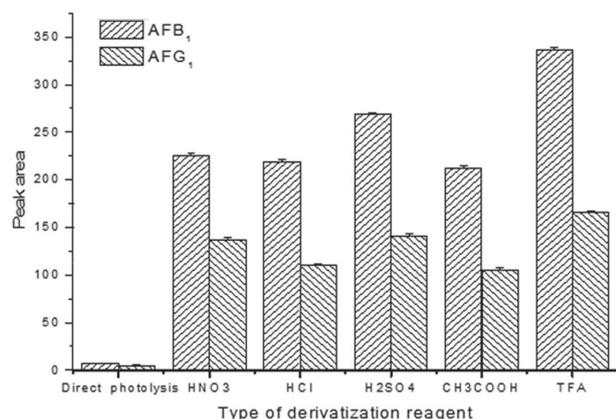
Figure 7. Derivatization efficiency of different kinds of derivatization reagent.

Effect of reaction temperature, UV radiation time and amount of TFA

The 3D response surface and 2D contour plots in Figure 8 provide a method to visualize the relationship between responses and experimental levels of each variable and the type of interactions between two test variables. Figure 8a depicts the effect of UV radiation time and amount of TFA on the peak area. With a given amount of TFA, the peak area increased rapidly with increasing UV radiation time and reached a maximum value, followed by a decline with its further increase.

The interaction between reaction temperature and amount of TFA is shown in Figure 8b. With a definite reaction temperature, the peak area increased rapidly with the increase of the added amount of TFA and reached the highest value, and then no obvious variation for peak areas with the further increase amount of TFA were observed. Figure 8c reveals the interaction between reaction temperature and UV radiation time. The interaction between them displayed a negative effect on the peak area. Effect of reaction temperature on the peak area was not important to the case of UV radiation time. The optimal conditions obtained using the model were as follows: 120 μL of TFA added; reaction temperature of 25 °C; UV radiation time of 15 min. Under these conditions, the model gave predicted values of Y (peak areas) being 406 for AFB$_1$, 322 for AFG$_1$. Finally, we got the optimum derivatization procedure: (*i*) to a purified sample solution containing 20.00 ng mL^{-1} of four standard AFs mixture in a vial, 120 μL of TFA; (*ii*) the vial was sealed and placed under UV lamp for 15 min; (*iii*) after derivatization, the mixture was directed for HPLC analysis.

Method validation

Linearity, limits of detection and precision

Satisfactory linear relationships and good correlation coefficient (r ≥ 0.9960) were obtained in the range of 0.50-50.00 ng mL^{-1} for AFB$_1$ and AFG$_1$, 2.00-200.00 ng mL^{-1} for AFB$_2$ and AFG$_2$ when each point was evaluated over five replicates at the same concentration. The limits of detection (LODs) were determined by successive analyses of spiked matrices with decreasing amounts of every AF standard until a signal-to-noise ratio 3:1. They were estimated to be 0.0392 ng mL^{-1} for AFB$_1$, 0.2429 ng mL^{-1} for AFB$_2$, 0.0842 ng mL^{-1} for AFG$_1$ and 0.4556 ng mL^{-1} for AFG$_2$. Satisfactory relative standard deviations (RSDs) of the peak areas and retention times for AFB$_2$, AFG$_2$, AFB$_1$, AFG$_1$ derivatives are shown in Table 1.

Confirmation of the derivative products for aflatoxins

Typically, aflatoxins B$_1$ and G$_1$ are converted to the derivative aflatoxins AFB$_{2a}$ and AFG$_{2a}$ by pre-column derivatization to increase their fluorescence intensity in HPLC-FLD analysis. In a RP-HPLC-FLD, the peaks of AFB$_1$ and AFG$_1$ disappeared, whereas two new peaks appeared with a higher intensity, as shown in Figure 9. Chromatogram supported that the initial derivative reaction products of AFG$_1$ and AFB$_1$ are AFG$_{2a}$ and AFB$_{2a}$. As the result shown in Table 2, the fluorescence intensities
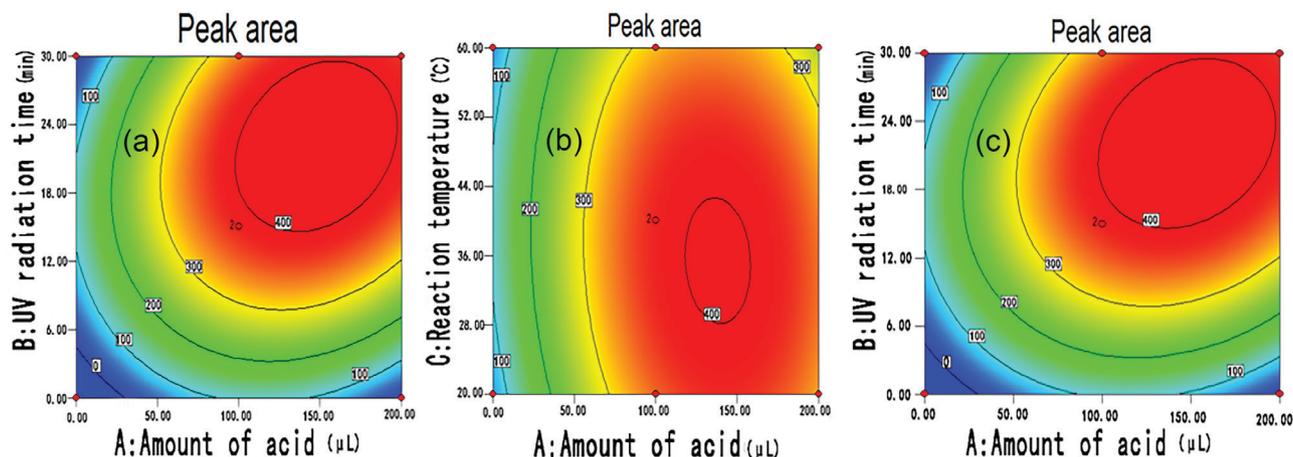
Figure 8. The 3D response surface and 2D contour plots of detection responses (peak area) affected by the amount of TFA (a), reaction temperature (b) and UV radiation time (c).

Table 1. Analytical features of the proposed method (n = 5)

Analyte	LR[a] / (ng mL^{-1})	Correlation coefficient (r)	LOD[b] / (ng mL^{-1})	LOQ[c] / (ng mL^{-1})	RSD[d] of retention time / %	RSD of peak area / %
AFB$_1$	0.50-100.00	0.9986	0.0392	0.1176	5.67	5.85
AFB$_2$	2.00-200.00	0.9991	0.2429	0.7287	2.89	3.89
AFG$_1$	0.50-100.00	0.9961	0.0842	0.2526	4.95	6.72
AFG$_2$	2.00-200.00	0.9989	0.4556	1.3668	3.88	4.78

[a]LR: linear range; [b]LOD: limit of detection; [c]limit of quantification; [d]RSD: relative standard deviation.
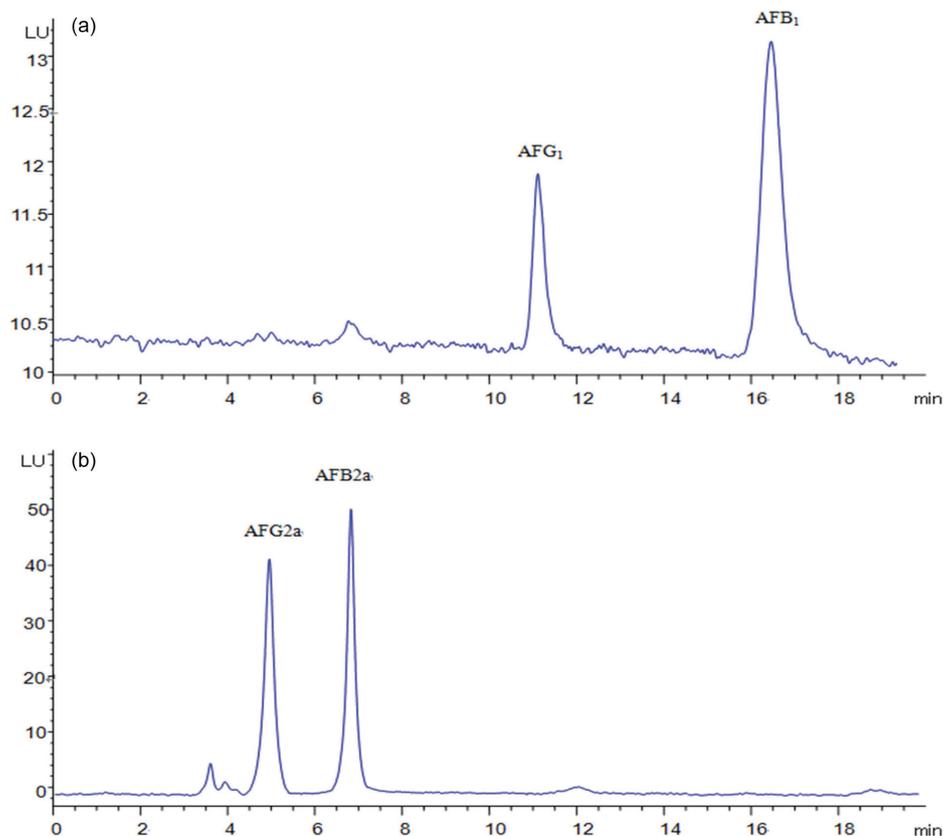
Figure 9. HPLC-FLD chromatograms of standard solutions of AFB$_1$ and AFG$_1$ (a) before and (b) after derivatization.

of AFB_{2a} and AFG_{2a} were significantly enhanced. The average fluorescence intensity enhancements were about 50 and 60 times of AFB_1 and AFG_1, respectively.

Table 2. Comparison of fluorescence intensities of aflatoxins B_1 (AFB_1) and G_1 (AFG_1) before or after pre-column derivatization

AFs	Concentration / ($ng\ mL^{-1}$)	Peak area before derivation	Peak area after derivation	Enhancement factor
	0.00	0	0	
	0.50	0	6.8	
AFB_1	5.00	0	71.9	50
	10.00	3.8	158.5	
	20.00	7.2	334.2	
	50.00	15.1	734.9	
	0.00	0	0	
	0.50	0	4.2	
AFG_1	5.00	0	40.2	60
	10.00	0	80.9	
	20.00	4.2	169.8	
	50.00	6.5	348.7	

Analyses of real samples

To evaluate the applicability of the proposed method in real matrices, it was applied to determination of four AFs in commercial feed samples. Recovery studies were carried out by spiking the samples with different concentration levels of the four AFs and the obtained results were summarized in Table 3. The acceptable recoveries in the range of 86.7 to 108.9% demonstrate that the matrix of feed sample was not affected on extraction efficiency of the analyte. Further examination of accuracy was performed by comparison of the results obtained from the proposed method and China's Nation Standard method (IAC-HPLC-FLD)[32] for determination of AFs in uncontaminated feed samples spiked with four target AFs at 20.00 ng g^{-1}. The results are summarized in Table 4. The statistical *t*-test analysis of the results showed that there are no significant differences between data obtained by the two methods at 95% confidence level.

Typical chromatograms obtained from the analysis of blank feed sample and spiked feed samples submitted to the proposed method and IAC-HPLC-FLD method were shown in Figure 10. The proposed method allowed a good separation among matrix components and the four aflatoxins in less than 10 min. Pre-column derivatization of AFs can increase detectability and/or selectivity of responses for the HPLC-FLD detector. By means of derivatization reaction, the non-fluorescent AFB_1 and AFG_1 are transformed into highly fluorescent hemiacetals B_{2a} and G_{2a}, and AFB_2 and AFG_2 are not affected by this derivatization due to their saturated structure.

Table 3. Results of assays to check the accuracy of the proposed method for aflatoxins AFB_1, AFB_2, AFG_1 and AFG_2 in three kinds of contaminated feed samples

Analyte	Spiked / ($ng\ g^{-1}$)	Feed for pig		Feed for chicken		Feed for fish	
		Found / ($\mu g\ kg^{-1}$)	Recovery / %	Found / ($\mu g\ kg^{-1}$)	Recovery / %	Found / ($\mu g\ kg^{-1}$)	Recovery / %
	0.00	2.12	–	ND[a]	–	3.42	–
AFB_1	10.00	11.29	91.7	10.13	101.3	13.45	100.3
	20.00	19.65	87.6	18.95	94.7	22.76	96.7
	50.00	46.87	89.5	47.44	94.8	50.12	93.4
	0.00	ND[a]	–	2.25	–	3.58	–
AFB_2	10.00	9.43	94.3	10.96	87.1	12.67	90.9
	20.00	18.22	91.1	19.89	88.2	21.22	88.2
	50.00	47.12	94.2	48.76	93.0	49.88	92.6
	0.00	ND[a]	–	ND[a]	–	ND[a]	–
AFG_1	10.00	8.99	89.9	8.99	89.9	108.9	108.9
	20.00	17.98	89.9	18.65	93.3	17.93	89.7
	50.00	47.23	94.5	47.87	95.7	46.86	93.7
	0.00	ND[a]	–	ND[a]	–	ND[a]	–
AFG_2	10.00	8.85	88.5	9.21	92.1	95.9	95.9
	20.00	17.33	86.7	18.75	93.8	18.12	90.6
	50.00	46.25	92.5	46.44	92.9	48.56	97.1

[a]ND: not detected.

Table 4. Comparison of aflatoxins (AFs) analyses in spiked feed samples by the proposed and standard IAC-HPLC-FLD method

Analyte	Spiked / (ng g^{-1})	Found amounts of analytes / (ng g^{-1})		Recovery / %	
		This method	IAC-HPLC-FLD method[a]	This method	IAC-HPLC-FLD method[a]
AFB$_1$	20.00	21.57 ± 1.0	17.57 ± 1.0	107.9	87.9
AFB$_2$	20.00	18.50 ± 1.0	18.79 ± 1.0	92.5	94.0
AFG$_1$	20.00	18.23 ± 1.0	17.23 ± 1.0	91.2	86.2
AFG$_2$	20.00	17.56 ± 1.0	17.82 ± 1.0	87.8	89.1

[a]Analysis by the immunoaffinity column-high-performance liquid chromatography with fluorescence detection (IAC-HPLC-FLD) method.[30]
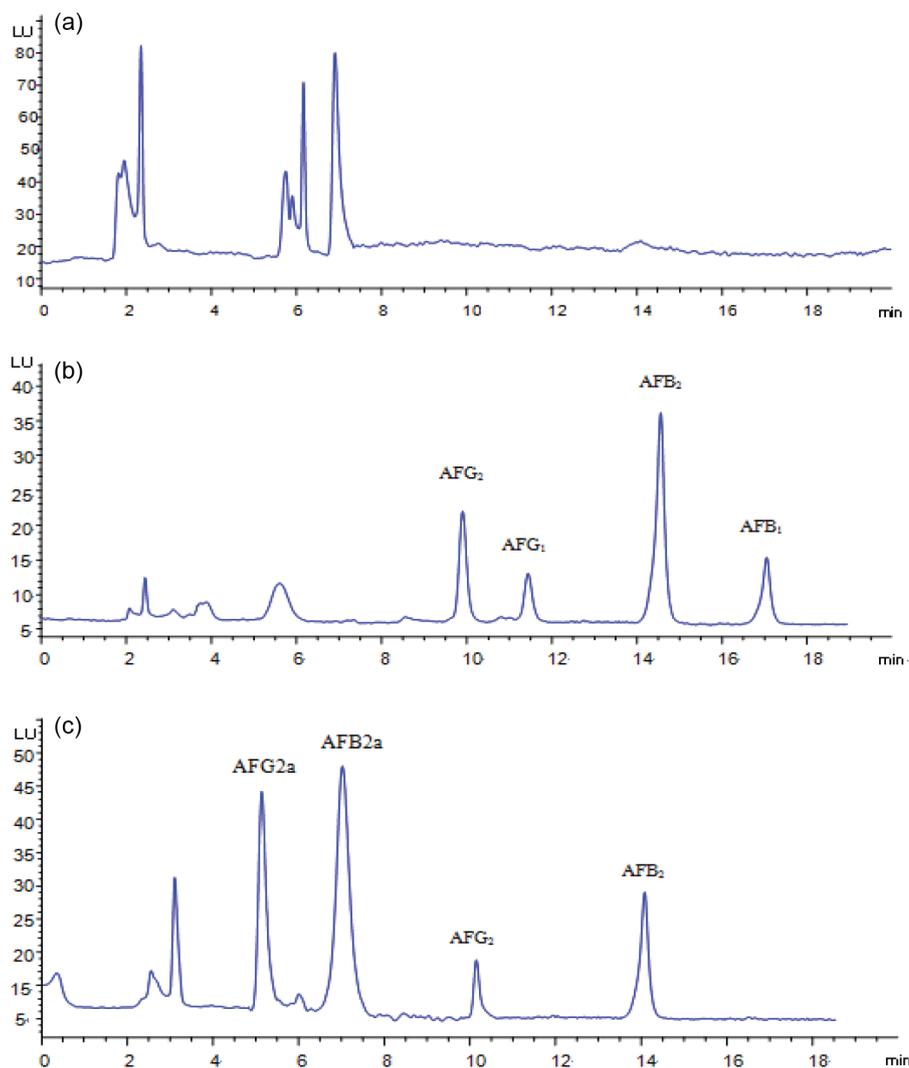
Figure 10. HPLC-FLD chromatograms relevant to (a) blank feed sample solution without pretreatment; (b) the spiked feed sample determined by IAC-HPLC-FLD method and (c) the spiked feed sample determined by the proposed method. The spiked concentrations of AFB$_1$, AFB$_2$, AFG$_1$ and AFG$_2$ were 20 ng mL^{-1}.

Comparing with other methods

In comparison with other pretreatment methods, the proposed method based on magnetic nanoparticles and magnetic separation technique used less adsorbent and shorter cleanup time. The cleanup efficiency demonstrated that PVP@Fe$_3$O$_4$ NPs can be used as a promising adsorbent for rapid and effective purification of feed samples prior to AFs determination. Moreover, AFs could be derived by coupling chemical derivatization with photochemical derivatization after purification, and lots of studies have been carried out in recent years. The proposed derivative method based on TFA and UV light was compared with other derivative methods as listed

Table 5. Comparison of current method characteristics with those of previously developed methods for derivatization and determination of AFs

Assay type	Derivatization method	Pretreatment time	LOD / (ng mL^{-1})	Recovery / %	Reference
LC-MS/MS[a]	–	1 h	0.09-0.38	90-105	31
ICA-HPLC-FLD[b]	bromine derivatization	1 h	0.4-0.8	86-89	32
SPE HPLC-PD-FLD[c]	photochemical derivatization	40 min	0.035-0.2	85.6-95.5	12
ICA-HPLC-FLD[b]	TFA derivatization	50 min	0.002-0.7	86-93	33
MSPE-HPLC-FLD[d]	TFA + UV light derivatization	20 min	0.127-0.632	89.2-109.7	this work

[a]LC-MS/MS: liquid chromatography tandem mass spectrometry; [b]ICA-HPLC-FLD: immunoaffinity column cleanup with high-performance liquid chromatography-fluorescence detection; [c]SPE-HPLC-PD-FLD: solid-phase microextraction coupled with high-performance liquid chromatography and post-column photochemical derivatization-fluorescence detection; [d]MSPE-HPLC-FLD: solid-phase microextraction coupled with high-performance liquid chromatography and fluorescence detection. LOD: limit of detection; TFA: trifluoracetic acid.

in Table 5. It revealed that the developed method had higher enrichment factor and similar LODs with the listed methods.[12,33-35] Furthermore, the new derivative method has distinct advantages in terms of good sensitivity at the high group selectivity, simplicity of instrumentation, and cost-effectiveness.

Conclusions

In this study, a novel PVP@Fe$_3$O$_4$ NPs sorbent was prepared, characterized, and applied in the cleanup procedure for determination of four trace-level AFs in animal feed samples. The PVP@Fe$_3$O$_4$ NPs tested has similar cleanup result with immunoaffinity columns, but it is cheaper and more maneuverable. As a result, the animal feed samples can be purified sufficiently with less matrix effect on HPLC detection. Furthermore, the purified extract was then derivatized with a combination of TFA and UV light, which allowed an obvious increase of the fluorescence intensities of AFB$_1$ and AFG$_1$ without needing electrochemical bromination apparatus or photochemical reactor. Work is currently in progress to extend the application of the proposed approach to other real matrices, and the advantages of rapidity, simplicity, ease of operation, and environmental protection enable an effective and smooth transfer to routine laboratories. Meanwhile, this method exhibits powerful potential for the trace analysis of AFs from feed, foodstuff and other complex samples.

Acknowledgments

References

1. Sweeney, M. J.; Dobson, A. D.; *Int. J. Food Microbiol.* **1998**, *43*, 141.

2. Creppy, E. E.; *Toxicol. Lett.* **2002**, *127*, 19.

3. Varsavsky, E.; Sommer, S. E.; *J. Chromatogr. A* **2003**, *1011*, 49.

4. Hopkins, J.; *Food Chem. Toxicol.* **1989**, *27*, 549.

5. Stroka, J.; Van, O. R.; Anklam, E.; *J. Chromatogr. A* **2000**, *904*, 251.

6. Asis, R.; Barrionuevo, D. L.; Giorda, L. M.; Nores, M. L.; Aldao, M. A.; *J. Agric. Food Chem.* **2005**, *53*, 9274.

7. Scudamore, K. A.; Patel, S.; *Food Addit. Contam.* **2000**, *17*, 407.

8. Sheijooni-Fumani, N.; Hassan, J.; Yousefi, S. R.; *J. Sep. Sci.* **2015**, *34*, 1333.

9. Li, X.; Li, H.; Ma, W.; Guo, Z.; Li, X.; Li, X.; Zhang, Q.; *Food Chem.* **2018**, *257*, 1.

10. Wang, L.; Wang, Z.; Gao, W.; Chen, J.; Yang, M.; Kuang, Y.; Huang, L.; Chen, S.; *Food Chem.* **2013**, *138*, 1048.

11. Geiss, O.; Senaldi, C.; Bianchi, I.; Lucena, A.; Tirendi, S.; Barrero-Moreno, J.; *J. Chromatogr. A* **2018**, *1566*, 13.

12. Wang, X.; Qi, P.; Wang, X.; Zhang, Q.; Wang, Z.; Xu, X.; Xu, H.; Zhang, H.; Wang, Q.; *J. Sep. Sci.* **2017**, *40*, 2438.

13. Sun, S.; Yao, K.; Zhao, S.; Zheng, P.; Wang, S.; Zeng, Y.; Liang, D.; Ke, Y.; Jiang, H.; *J. Chromatogr. B* **2018**, *1092*, 228.

14. Yao, K.; Wen, K.; Shan, W.; Xie, S.; Peng, T.; Wang, J.; Jiang, H.; Shao, B.; *J. Chromatogr. B* **2018**, *1080*, 50.

15. Kaymak, T.; Türker, L.; Tulay, H.; Stroka, J.; *J. AOAC Int.* **2018**, *101*, 1839.

16. Wejdan, S. K.; Bahruddin, S.; Yan, C. B.; Norhasani, H.; Abdussalam, S. M. A.; Muhammadidiris, S.; Baharuddin, S.; *Food Chem.* **2010**, *118*, 882.

17. Li, X. L.; Tan, G. L.; Liang, B.; Liu, Y.; *Mod. Food Sci. Technol.* **2015**, *31*, 342.

18. Tamura, M.; Takahashi, A.; Uyama, A.; Mochizuki, N.; *Toxins* **2012**, *4*, 476.

19. Tejamaya, M.; Römer, I.; Merrifield, R. C.; Lead, J. R.; *Environ. Sci. Technol.* **2012**, *46*, 7011.

20. Hitchman, A.; Smith, G. H. S.; Ju-Nam, Y.; Sterling, M.; Lead, J. R.; *Chemosphere* **2013**, *90*, 410.

21. Tahmasebi, E.; Yamini, Y.; *Anal. Chim. Acta* **2012**, *756*, 13.

22. Golge, O.; Hepsag, F.; Kabak, B.; *Food Control* **2016**, *59*, 731.

23. Hepsag, F.; Golge, O.; Kabak, B.; *Food Control* **2014***, 38*, 75.

24. Tarter, E. J.; Hanchay, J. P.; Scott, P. M.; *J. - Assoc. Off. Anal. Chem.* **1984**, *67*, 597.

25. Liu, G.; Zhu, Z.; Cheng, J.; Senyuva, H. Z.; *J. AOAC Int*. **2012**, *95*, 122.

26. Roch, O. G.; Blunden, G.; Coker, R. D.; Nawaz, S.; *Food Chem*. **1995**, *52*, 93.

27. Beebe, R. M.; *J. - Assoc. Off. Anal. Chem.* **1978**, *61*, 1347.

28. Mirshahghassemi, S.; Lead, J. R.; *Environ. Sci. Technol*. **2015**, *49*, 11729.

29. *Design-Expert 7.1.3*; State-Ease, Inc., Minneapolis, USA, 2008.

30. Takahashi, D. M.; *J. Chromatogr. A* **1977**, *131*, 147.

31. Joshua, H.; *J. Chromatogr. A* **1993**, *654*, 247.

32. Ghali, R.; Belouaer, I.; Hdiri, S.; Ghorbel, H.; Maaroufi, K.; Hedilli, A.; *J. Food Compos. Anal*. **2009**, *22*, 751.

33. Cervino, C.; Asam, S.; Knopp, D.; Rychlik, M.; Niessner, R.; *J. Agric. Food Chem.* **2008**, *56*, 1873.

34. Senyuva, H. Z.; Gilbert, J.; *J. AOAC Int*. **2005**, *88*, 526.

35. Göbel, R.; Lusky, K.; *J. AOAC Int*. **2004**, *87*, 411.